Heart Surgery Forum 2023; 26(5): E498–E511
doi: 10.59958/hsf.5775

Article

Exploring the Common Gene Signatures Between Myocardial Infarction-Reperfusion Injury and the Gut Microbiome Using Bioinformatics

Xiao Jiang[1], Caiyun Li[1], Xuting Xia[1], Jiangbo Tong[2], Jin Cheng[3], Xinhui Li[1,*]

[1]College of Traditional Chinese Medicine, Hunan University of Chinese Medicine, 410208 Changsha, Hunan, China
[2]Graduate School, Yangzhou University, 225009 Yangzhou, Jiangsu, China
[3]Department of Pediatric Intrarenal and Rheumatology Immunology, The Affiliated Hospital of Xuzhou Medical University, 221000 Xuzhou, Jiangsu, China
*Correspondence: 003760@hnucm.edu.cn (Xinhui Li)

Submitted: 24 May 2023 Revised: 4 September 2023 Accepted: 11 September 2023 Published: 15 October 2023

Abstract

Background: This bioinformatics report attempts to explore the cross-talk genes, transcription factors (TFs), and pathways related to myocardial ischemia-reperfusion injury (MIRI) as well as the gut microbiome. **Method**: The datasets GSE61592 (three MIRI and three sham samples) and GSE160516 (twelve MIRI and four sham samples) were selected in the Gene Expression Omnibus (GEO) database. Differentially expressed genes (DEGs) identification ($p < 0.05$ and |log FC (fold change)| $\geq$1) together with functional annotation ($p < 0.05$) was implemented. The Cytoscape platform established the protein-protein interaction (PPI) network. Genes associated with gut microbiome disorder were extracted based on the DisGeNET database, and those associated with MIRI were overlapped. The Recursive Feature Elimination (RFE) algorithm was adopted for selecting features, and cross-talk genes were predicted by the Support Vector Machine (SVM) models. A network encompassing cross-talk genes along with the TFs was thereby established. **Result**: The MIRI datasets comprised 138 shared DEGs, with 101 showing up-regulation whereas 37 showing down-regulation. Notably, the PPI interwork for MIRI contained 2517 edges along with 1818 nodes. By using RFE and SVM methods, six feature genes with the highest prediction were identified: *B2m*, *VCAM-1*, *PDIA4*, *Ptgds*, *Mlxipl*, and *ACADS*. Among these genes, *B2m* and *PDIA4* were most highly expressed in MIRI and the gut microbiome disorder. **Conclusion**: *B2m* and *PDIA4* were identified to be significantly correlated with candidate cross-talk genes of MIRI with gut microbiome disorder, implying a similarity between MIRI and Gut microbiome disorder (GMD). These genes can serve as an experimental research basis for future studies.

Keywords

myocardium ischemia-reperfusion injury; gut microbiome disorder; bioinformatics; cross-talk genes; *B2m*; *PDIA4*

Introduction

Myocardial ischemia occurs when the heart receives reduced blood flow. Myocardial Ischemia- reperfusion may induce reperfusion injury (MIRI), which can reduce the clinical benefits of revascularization if not treated on time [1]. MIRI mainly presents in various forms, further aggravating structural and functional cardiac damage, eventually causing adverse cardiovascular outcomes [2]. Therefore, MIRI has become the most common clinical problem of acute myocardial infarction (AMI) after interventional or thrombolytic therapy [3]. Mechanisms contributing to MIRI are related to inflammatory reaction, immune reaction, unfolded protein reactions (UPR), endoplasmic reticulum (ER) stress, oxidative stress (OS), cell death, or alteration of long non-coding RNAs (lncRNA) levels [4,5]. This mechanism is unclear. Hence, further study is warranted [6,7].

As revealed by metagenomic analysis and genome sequencing, gut microbiome disorder (GMD) may affect coronary artery disease (CAD) [8,9]. Manipulating gut microbiome composition affects the cardiovascular condition of the host [10,11]. In addition, the gastrointestinal tract can be viewed as a diverse and enormous ecosystem that produces a considerable amount of microbial metabolites. Such substances can be absorbed into the circulation and serve as mediators of gut microbial effects on the host. Hence, the gut microbiota contributes directly or indirectly to our immune status. Generally, microbiome contributes directly or indirectly to CAD. Inflammation and lipid metabolism disorders have important effects on measuring the severity and development of a disease [12,13]. There is a controversy regarding the causal relationship be-

© 2023 Forum Multimedia Publishing, LLC.

Publisher's Note: Forum Multimedia Publishing stays neutral with regard to jurisdictional claims in published maps and institutional affiliations.

tween CAD and GMD [14]. According to several studies, metabolic and inflammatory pathways mediated by gut microbiota may be the potential mechanisms to investigate [15–18].

In recent years, gene chip expression mining data using bioinformatics technology has been widely used to analyze related differentially expressed genes (DEGs). The technique has enabled interlinking between rheumatoid arthritis (RA) and periimplantitis, and carotid atherosclerosis and periodontitis [19,20]. DEGs provide valuable clues to explore the development and prevention of pathological processes in MIRI and GMD. Therefore, the present work applied bioinformatics analysis for revealing the transcriptomic cross-talk mechanisms in MIRI with the gut microbiome. Cross-talk genes in MIRI with the gut microbiome might be present. These genes maintain similarities between the two states and establish an autoinflammatory character caused by gut microbiome disorders.

Material and Methods

Databases and Study Design

Two MIRI datasets collected in Gene Expression Omnibus (GEO) were included, i.e., GSE61592 and GSE160516, which were selected using criteria described below. Datasets included determined MIRI samples representing the MIRI group, and sham samples were the controls. All samples were taken from mice. Three controls and three MIRI samples were included from GSE61592, while twelve MIRI samples and four sham samples in GSE160516 were used for controls. Fig. 1 displays our analytical flowchart.

Differentially Expressed Genes (DEGs) Identification

By adopting the R software Microarray (Auckland, New Zealand) limma package, Linear Models were applied to assess differences between sham and MIRI groups. First, the expression data were annotated, and the probe matrix was converted into a gene matrix. Genes satisfying $p < 0.05$ and $|\log FC \text{ (fold change)}| \geq 1$ were deemed to be DEGs. Those shared DEGs with up/down-regulation between GSE61592 and GSE160516 were adopted in further analyses after excluding the uncommon DEGs. A valid linear model was employed for "limma" analysis. Those missing values were filled in as the genes of multiple probes to correct the data. The processed gene expression data were applied after fitting each gene to a linear model. The differential gene analysis results were inferred from the empirical. Bayes estimation methods that weighted the least squares method, moderate t-statistics, F statistics, and differential expression values. These methods improved the inference of small experiments at the gene as well as the gene-set level.

Functional Annotation

Our analysis was carried out based on previous studies. Therefore, those biological activities enriched by those identified DEGs, either with up-regulation or down-regulation, were analyzed. $p < 0.05$ was considered a significant functional enrichment. Ten of the most significant GO Biological Processes (BP), Molecular Functions (MF), and Cell Components (CC) were sorted out based on the increasing p-values after selecting each enriched pathway. GO and KEGG analysis of differential genes was performed using the DAVID database. The results were visualized with the ggplot2 package for R.

Protein-Protein Interaction (PPI) Network Establishment

PPIs were extracted after uploading the common targets to the STRING tool and constructing a PPI network. DEGs were uploaded using STRING (https://cn.string-db.org/). Cytospace was adopted for result visualization, and key genes were identified using cytoHubba (Cytospace version 3.9.1).

Identification of probably Cross-Talk Genes

The gut microbiome disorder genes were obtained from the gutMGene database (http://bio-annotation.cn/gutmgene/search.dhtml) and Mouse Genome Informatics (http://www.informatics.jax.org/). Those probably cross-talk gut microbiome disorder genes, overlapping with MIRI-associated DEGs, were obtained to construct the cross-talk gene-associated PPI network.

Transcription Factor (TF)-Mediated Cross-Talk Genes

TF-target gene regulatory pairs were obtained in the ChEA 3 database (https://maayanlab.cloud/chea3/). MIRI-associated TF-target pairs were obtained in line with TF-target relation, followed by establishment of TF-target gene interaction network as well as network visualization with Cytoscape.

Support Vector Machine (SVM) Modeling Based on Cross-Talk Gene Feature Selection

Gene expression profiles from the GSE61592 and GSE160516 datasets were combined. The ComBat approach based on the SVA packages of the R software was utilized for batch correction of combined data. Intersecting gene expression data from those above two datasets were identified by eliminating the batch effect. Gene levels acquired following eliminating the batch effect changed compared with their initial levels in both datasets. The Scale approach in R was adopted for standardizing resultant data, followed by establishment of the SVM model. Initial expression profiles of both datasets, GSE61592 and

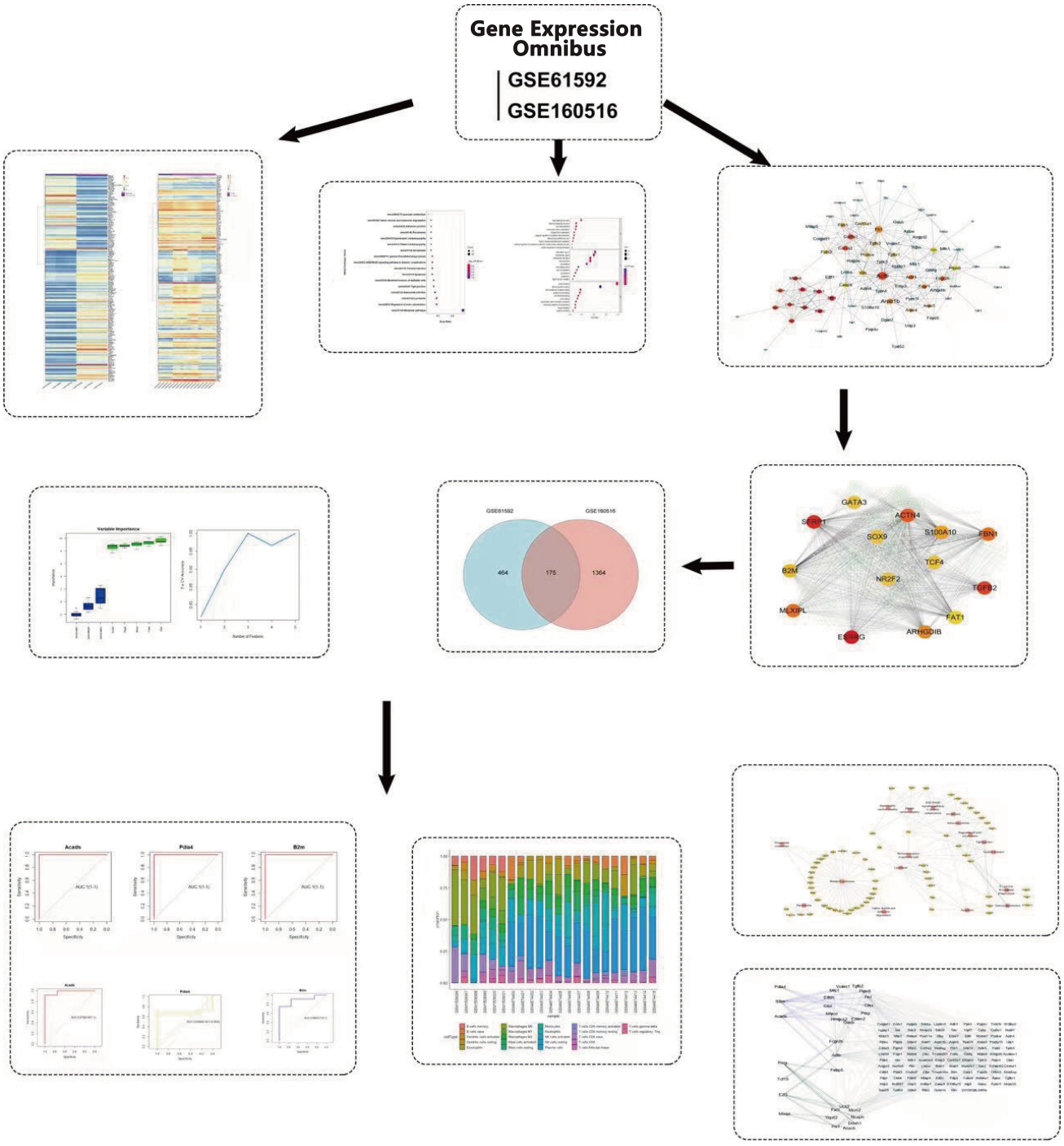

Fig. 1. The flow-process of the current study. Exploring the common gene between Myocardial Infarction-Reperfusion Injury and the Gut Microbiome.

GSE160516, were acquired for direct standardization using Scale. Candidate cross-talk gene levels were acquired based on combined data. The conventional Recursive Feature Elimination (RFE) algorithm and R software Boruta algorithm were utilized for feature selection. The receiver operating characteristic (ROC) curves were subsequently plotted to evaluate prediction using the pROC package, whereas the R software ggplot2 package was adopted for visualization.

Immune Infiltration Method

The cell marker gene set for immune cells was obtained from Newman *et al* . [21]. The 175 differential genes were uploaded to the CIBERSORTx (https://cibersortx.stanford.edu/) online platform. The results were visualized using default parameters on the ggplot2 and ggpubr packages.

Pathway Enriched by Cross-Talk Genes

The significantly enriched pathways were identified by DEGs of MIRI. The potential cross-talk pathways, probably bridging GMD and MIRI, were chosen. Then, the directed network was developed: G = (V, E), in which V represents gene sets associated with the pathway, whereas E indicates pathway-gene interaction. Genes involved in all pathways were acquired. Cytoscape was then utilized to build the pathway-cross-talk gene network. In G = (V, E), Vr indicates GMD-associated genes, while Vp depicts DEGs related to MIRI, which included candidate cross-talk genes.

Cross-talk genes were obtained from pathway–gene pairs, and TFs targeting cross-talk genes were also acquired. Additionally, MIRI-associated DEGs interacting with pathway-gene pairs-related cross-talk genes were identified. Every DEG of MIRI is expressed as Vp in that network, TFs are expressed as VTF, while candidate cross-talk genes are expressed as Vct. Finally, relations across MIRI-associated genes, TFs, and cross-talk genes were established.

Results

DEGs of MIRI

Comparison between GSE61592 and GSE160516 revealed 175 common DEGs (Fig. 2A,B).

Functional Annotation

DEGs remarkably associated with BPs showed the closest relation with the metabolic pathway, regulation of actin cytoskeleton, lysosomes, and Salmonella infection (Fig. 3A). Fig. 3B displays corresponding biological functions involving the DEGs.

PPI Network

Our established MIRI-related PPI network included 148 nodes together with 748 edges (Fig. 4). The top 30 nodes were identified after analyzing the topological network characteristics of the PPI network. Genes Actb, Fn1, and Col3a1 displayed the highest degree of cross-talk in the biological network. Hence, these genes probably affect the development of MIRI.

TF-Gene Regulatory Network

11,861 TF-target interactions were obtained, which were adopted for the construction of the TF-target network (Fig. 5). The most significant candidate cross-talk genes included *SFRP1*, *ESRRG*, and *TGFB2*. Consequently, these genes might have a critical effect on the TF-target network. A Venn diagram for DEGs is expressed in Fig. 6.

Table 1. SVM-REF predict value.

Gene Name	Feature ID	Average Rank
ACADS	1	1.533333
PDIA4	4	3.000000
B2 m	2	3.133333
Mlxipl	3	3.600000
Ptgds	5	3.733333

SVM-REF, support vector machine-recursive feature elimination; ID, identification.

Prediction of Risk Cross-Talk Genes

Normalized results were classified. Boruta and RFE algorithms verified the results and selected the features (Fig. 7A,B). A total of three genes (*B2m*, *PDIA4*, and *ACADS*) showing the highest prediction were selected from the intersection results. RFE features were chosen to conduct later analyses. Three feature gene levels were extracted based on combined results. A five-fold cross-validation (CV) was applied in obtaining the optimal hyperparameters for the SVM model(s). Thus, a SVM model was built with these three genes (Table 1).

Predicting the Relationship between MIRI and the Gut Microbiome

B2m and *PIDA4* genes displayed the highest expression in MIRI and GMD (Fig. 8A–C). Values of area under the curve (AUC) for *B2m* and *PIDA4* of the MIRI dataset (GSE61592) were over 95% (Fig. 8D–F). The AUC values of *B2m* and *PIDA4* in the GMD dataset (GSE160516) were 89.6% and 68.8%, respectively.

Immune Infiltration Analysis

Immune landscapes of MIRI and Gut Microbiome (GM) were changed in comparison with control (Fig. 9). Correlation analysis depicted two crucial cross-talk genes from the stacking bar graph. In this heat map, red represents a positive correlation, and blue represents a negative correlation, the numerical value represents the correlation coefficient. If it is positive, it indicates a positive regulatory relationship between the gene and the immune cell, while a negative value indicates a negative regulatory relationship. The correlation index and *p*-value are calculated using the Spearman test. The *B2m* and *PIDA4* are positively correlated with various immune cells, such as naive B cells, Plasma cells, memory activated T cells CD4, activated NK cells, M2 Macrophages, resting Dendritic cells, Eosinophils and Neutrophils. The Acads is positively correlated with various immune cells, such as memory B cells, CD8 T cells, memory resting T cells, memory resting CD4 cells, regulatory T cells (Tregs), gamma delta T cells, resting NK cells, Monocytes, M0 Macrophages, activated Dendritic cells, resting Mast cells, and Neutrophils.

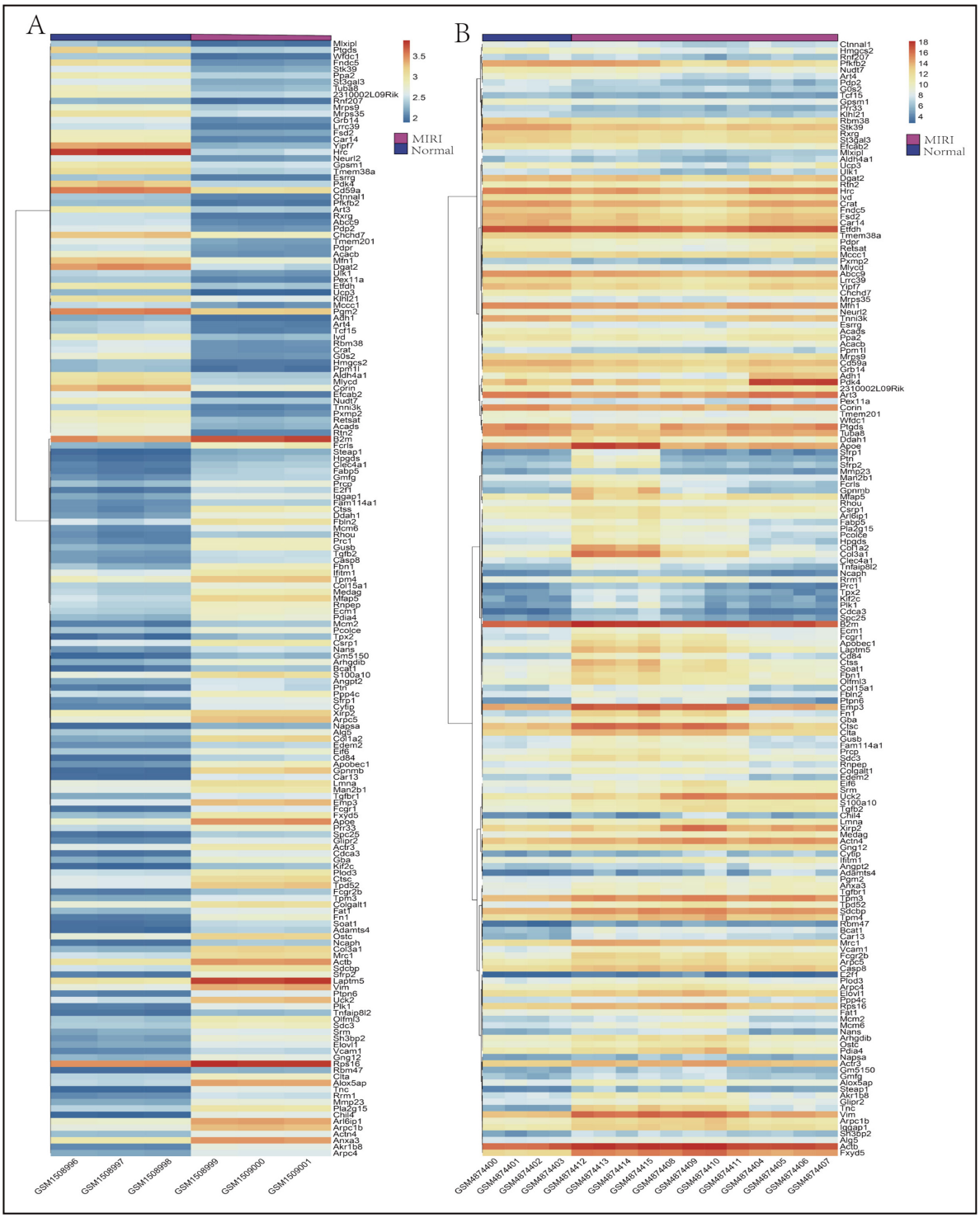

Fig. 2. The expression level of 175 common DEGs in (A) GSE61592 and (B) GSE160516 datasets. DEGs, differentially expressed genes.

Pathway-Gene Functional Network

Finally, 17 significantly enriched pathways, possibly vital for developing MIRI, were selected. Cross-talk between MIRI and GM was identified by constructing a pathway-gene cross-talk network, which included 79 nodes along with 125 edges (Fig. 10).

TFs modulation within cross-talk pathways in MIRI with GMD was studied by extracting TFs in TF-target relations as well as cross-talk genes in those activated pathways. In the meantime, cross-talk gene PPIs were obtained to build an activated TF-cross-talk gene network (Fig. 11). As discovered, TFs modulated the cross-talk genes.

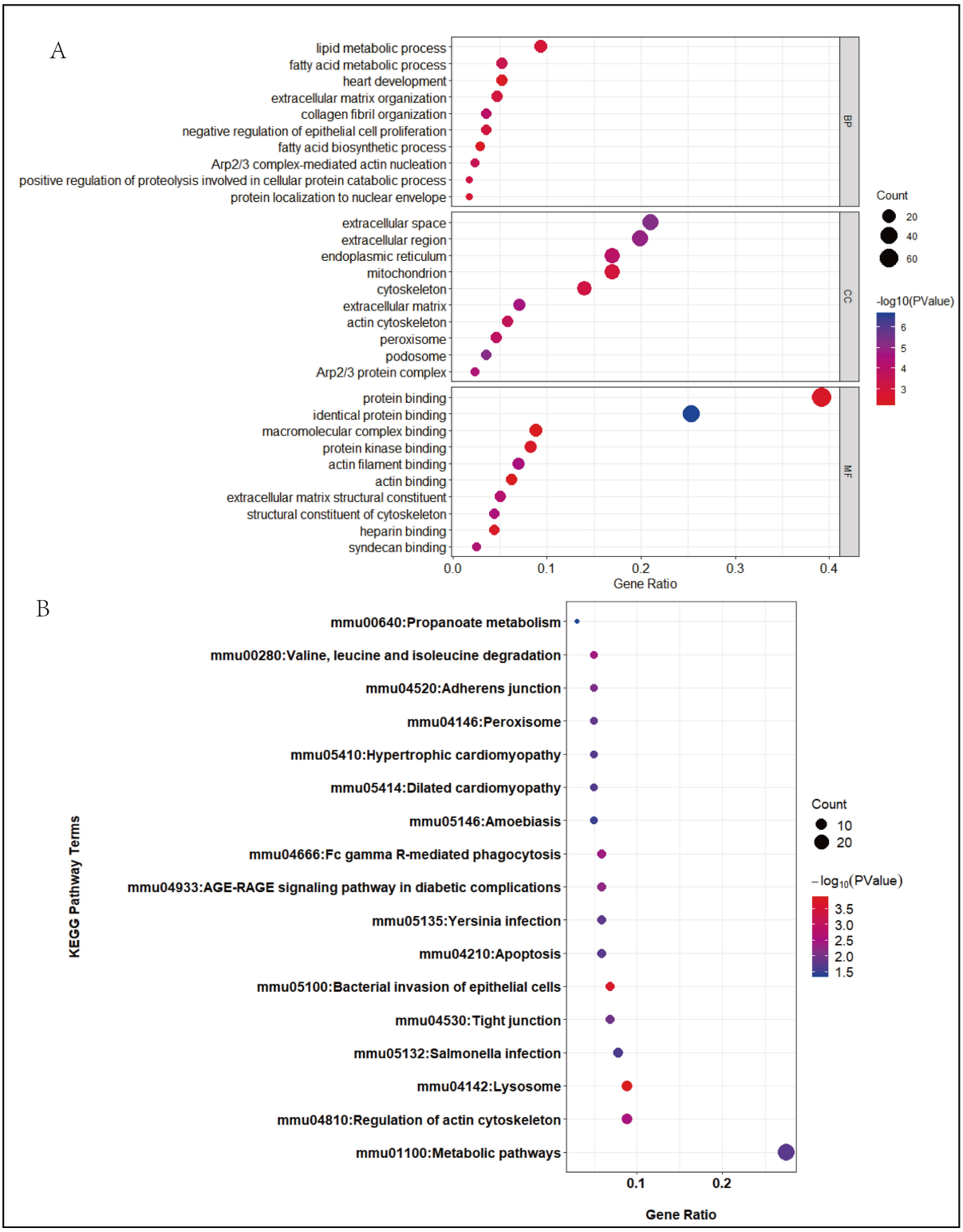

Fig. 3. The significantly enriched (A) biological pathways and (B) functions of the 178 common DEGs.

Discussion

This study focused on exploring cross-talk of MIRI with GMD by bioinformatics analysis. Consequently, *B2m*, *PDIA4*, and *ACADS* were identified as closely related genes, and some associated pathways were also found. These genes were relevant in MIRI and GMD, considering the associated predicting performances and expression levels in such diseases. Furthermore, the ROC values of *B2m* and *PDIA4* were higher than those of other genes. Hence, they were highly correlated. Moreover, *PDIA4* interacted

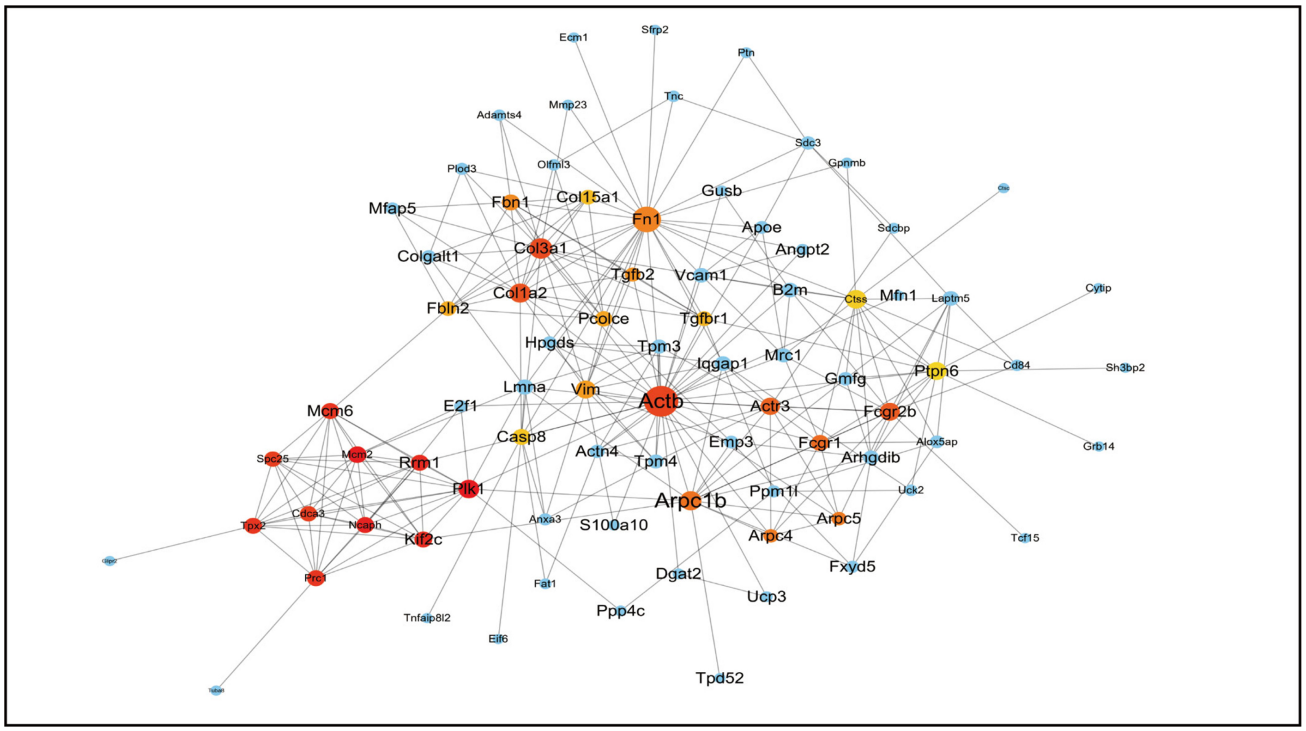

Fig. 4. The protein-protein interaction network of the hub genes.

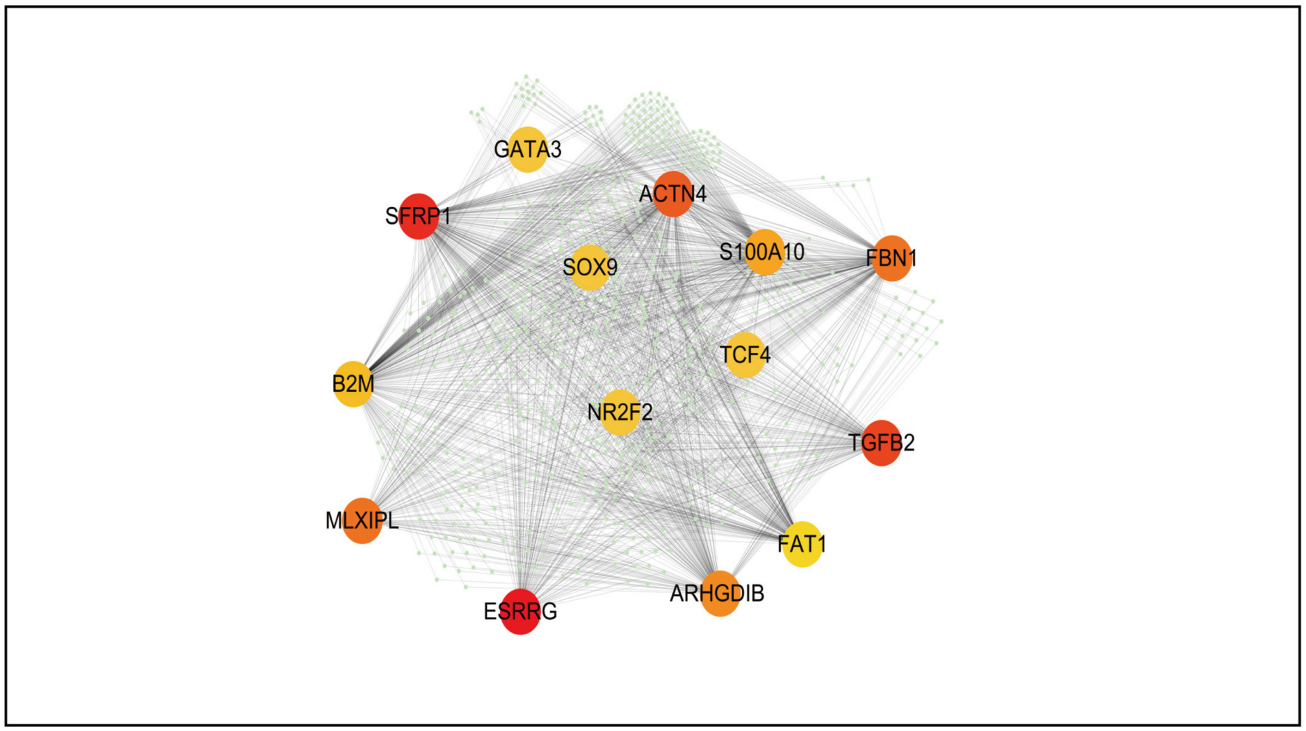

Fig. 5. The TF-target network of hub genes. TF, transcription factors.

with *Vcam1*, indicating the likely relation of *PDIA4* with GMD by interaction with additional genes. Therefore, our work concentrates on the connection between these results despite some ambiguity.

This work obtained MIRI datasets in two works examining RNA expression of MIRI and sham samples [22]. It is challenging to compare MIRI and GMD because a concrete conclusion has not been found. Universally, MIRI is regarded as a complex disease whose pathogenesis needs further investigation. A heterogenic flora of potential pathogens was previously considered essential for causing inflammation. Nevertheless, genetic predisposi-

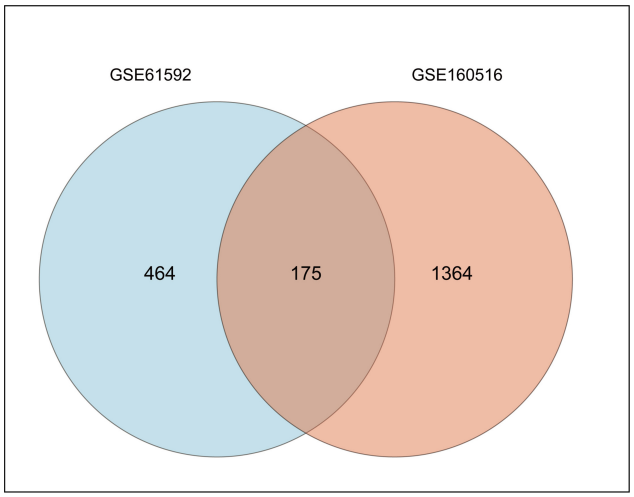

Fig. 6. Venn diagram of DEGs.

tion amongst various immunological responses is highly relevant in the occurrence of MIRI. Consequently, the immune response driven by the microbiome of MIRI is complex. The gut microbiome comprises a heterogeneous and varied microbial composition. A possible gut microbiome disorder increases the complexity of the MIRI tissues. The disruption of the gut flora is essential for GMD and the immune response. Because of different microbial and associated pathways, the significance of this work cannot be easily determined. Host-produced bioactive substances are another class of related clinical indicators. Commensal microbes modulating the MIRI-related metabolic factors are also important. Urolithin B can be obtained in ellagitannins through the components of gut microbial. It affects the expression of genes related to RCT while increasing macrophage cholesterol efflux in HDL particles, consequently restraining intra-plaque lipid deposition [23]. A population-based cohort study confirmed that metabolic risks are associated with microbial functional factors. For example, lipoprotein particle composition, carbohydrate/sugar derivative metabolism, as well as fatty acid saturation can predict adverse CVD events [24]. Therefore, the potential link between MIRI and GMD can be based on similar risk factors.

Specifically, a lipid metabolism disorder potentially mediates obesity progression and affects inflammatory pathogenesis. The condition also affects *PDIA4* and inflammatory factors like IL-6 and TNF-α [25]. *PDIA4* was more critical than the other genes identified by our results. Thus, relevant exposure risk factors such as lipid metabolism disorders need to be reconsidered. Additional elements, such as comorbidities like diabetes mellitus, would be interlinked. Diabetes mellitus increases CVD and GMD risks [26,27]. In addition, *PDIA4* existing onto cell membrane appears to perform the new cross-talk function of interacting with additional signaling factors while activating those unidentified intracellular pathways. For example, *PDIA4* can interact with extracellular cytokines while counteracting neutrophil infiltration mediated by cytokines. It also counteracts the maturation of thyroglobulin associated with oxidoreductases [28,29]. The complexity of the issue is increased by considering exposure risk factors (like lipid metabolism disorders) and comorbidities (like diabetes mellitus). Studies like ours indicate the ambiguity in the relevant pathways, and additional investigation is warranted.

In the human body, there is a symbiotic relationship of gut microbiota, which is crucial to determining our health. The immune system continually defends against pathogens when stimulated by associations of gut microbiota with intestinal cells regulating barrier activities [30]. For example, host intestinal cells directly interact with structural components of the microbiota in response to a foreign body. This reaction is similar to that produced when TLRs recognize cardiovascular damage, often in damage-associated molecular patterns (DAMPs) or alarmins [31]. Accordingly, gut microbiota is considered to be the prolific endocrine organ that produces excessive humoral molecules via the metabolism-independent or -dependent pathways, which induce innate immune reactions [32]. Therefore, there may be a similar mechanism with cardiovascular damage, as noted by cross-talk genes as well as common pathways based on our results.

B2m was the most significant cross-talk gene identified in this work. It is responsible for encoding one serum protein related to a class I heavy chain of major histocompatibility complex (MHC) on many nucleated cell surfaces. That encoded antimicrobial protein displays antibacterial effects within amniotic fluid. Previous studies associated *B2m* with cardiac performance [33]. Additionally, *B2m* is related to inflammation [34]. It has been reported that Trimethylamine-oxide (TMAO) is a major contributor to the development of atherosclerosis. Such a substance augments inflammatory and endothelial dysfunction. These reports support the view that *B2m* are critical targets of TMAO-induced endothelial dysfunction and prevention of atherosclerosis by mitigating the inflammatory response. Another study has demonstrated the role of *B2m* in predicting the prevalence of atherosclerosis, such as intimal hyperplasia or asymptomatic carotid artery plaque [35]. *B2m* is not always a sensitive predictor of adverse events in some conditions [36]. However, *B2m* is undeniably associated with cardiac function and atherosclerosis [37]. Upon ischemic injury, *B2m* is highly expressed and secreted in cardiomyocytes. Collecting gene levels in major myocardial cells in diverse time periods following ischemic injury can describe differences in cells and transcription. Alterations of cell activities in cardiac remodeling were demonstrated by single-cell transcriptomics [38]. MIRI can activate various molecular and cellular events to heal cardiac injury. These processes have an important role in determining patient outcomes [39]. Accord-

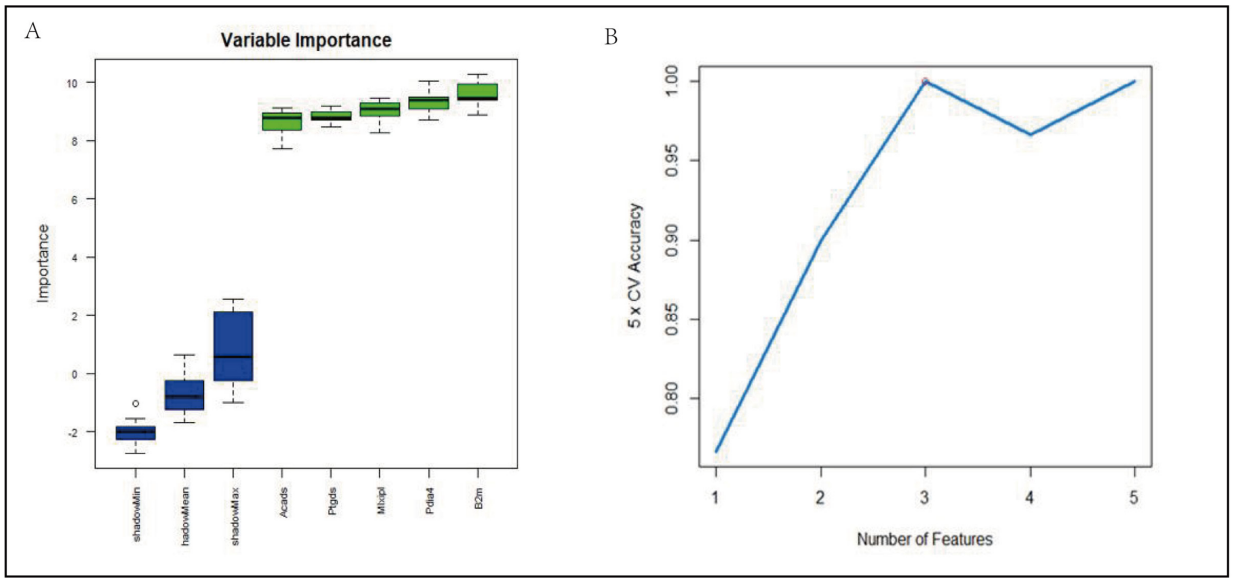

Fig. 7. Feature selection by algorithm. (A) Cross-talk genes selected using the Boruta algorithm. (B) Six feature genes selected using the RFE algorithm. RFE, recursive feature elimination.

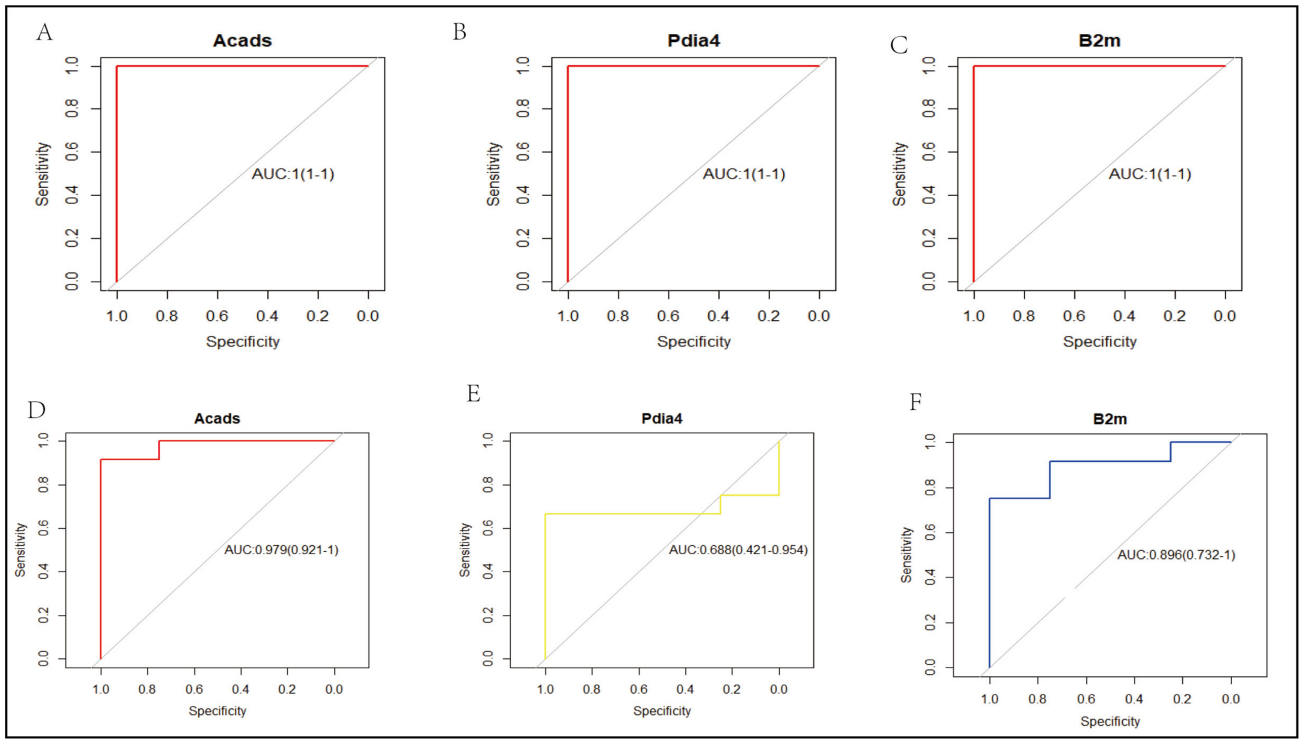

Fig. 8. ROC curve values of three genes. (A) The Acads ROC curve value calculate by GSE61592. (B)The *Pdia4* ROC curve value calculate by GSE61592. (C)The *B2m* ROC curve value calculate by GSE61592. (D) The Acads ROC curve value calculate by GSE160516. (E)The *Pdia4* ROC curve value calculate by GSE160516. (F) The *B2m* ROC curve value calculate by GSE160516. ROC, receiver operating characteristic.

ing to *in-vitro* experiments, *B2m* can stimulate wound healing by activating fibroblasts. Its signaling mechanism remains unexplored at present. Earlier reports indicate the involvement of secreted *B2m* in the fibrotic response in post-ischemic myocardial repair. This repair facilitates improvement of wound healing seen among treated rats [40]. *B2m* is a housekeeping gene (HKG), and its role in affecting bowel inflammation remains to be explored. Inflammatory bowel disease (IBD)-related chronic inflammation may induce colorectal cancer (CRC), while the cytokine-mediated

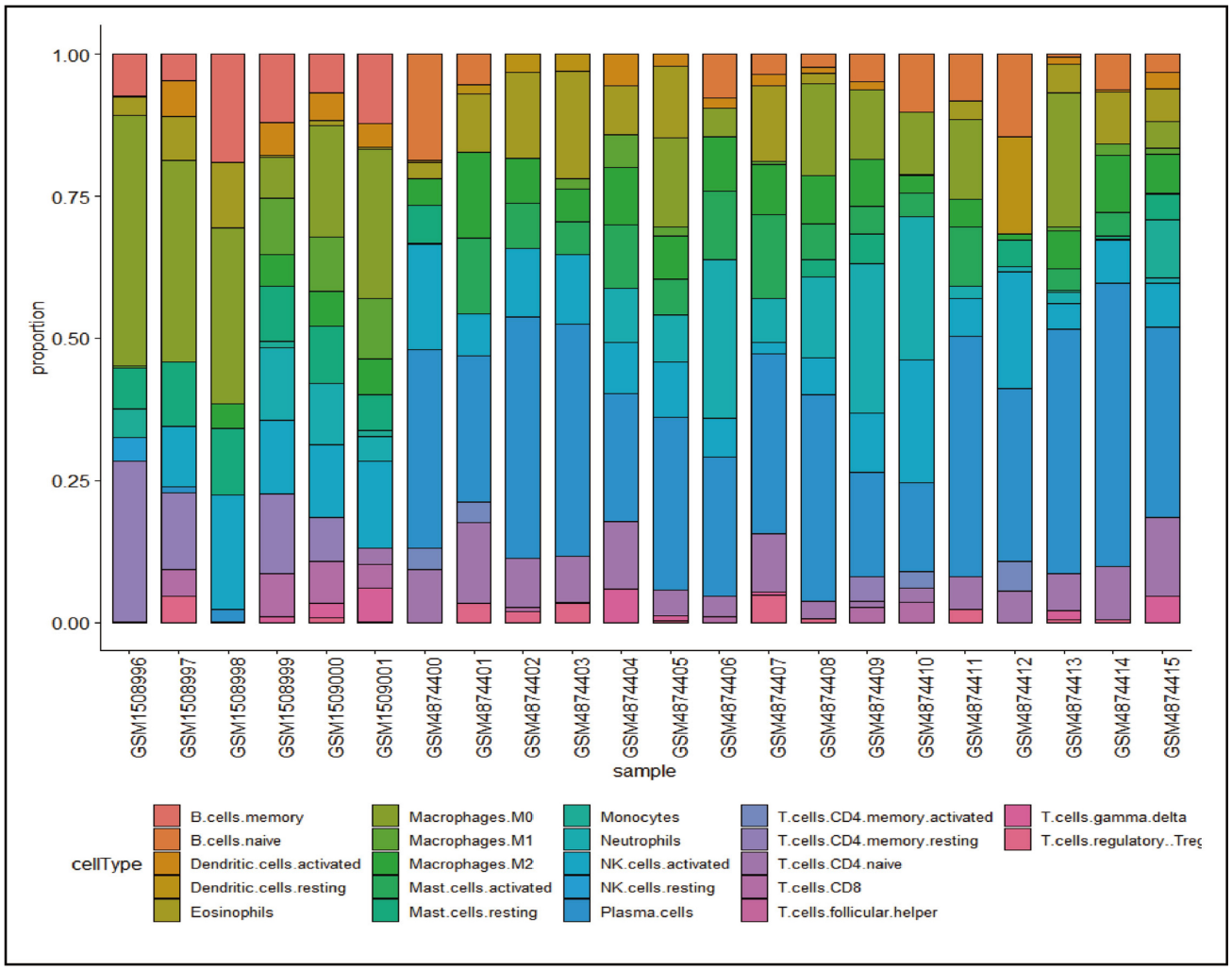

Fig. 9. Immune infiltration analysis bar graph.

changes of regulatory pathways can impact HKG levels similar to neoplastic transformation. In contrast, HKG levels can be affected by bowel inflammation, mainly being down-regulated, at a greater level than neoplastic transformation. During inflammation, *B2m* is significantly up regulated [41]. IBD shows a close relationship with imbalance of flora or metabolites in GMD. This pattern inevitably aggravates the instability of *B2m*. This instability, supposedly unregulated and hence used as a normalizer, affects the fibrotic response during myocardial repair in ischemia. Epidemiologic studies have revealed the correlation between the risk of cardiovascular events and mediators of inflammation. Intestinal barrier impairment disrupts host immune homeostasis. Multiple factors can lead to intestinal barrier function disruption, for instance, decreased intestinal perfusion in CVD effects the structure of the villi (and microvilli), which are susceptible to ischemia injury. *B2m* may have clinical value as a potential diagnostic biomarker.

PDIA4 is another closely related cross-talk gene. It encodes one disulfide isomerase (PDI) family member of the ER protein. *PDIA4* is responsible for catalyzing thiol-disulfide exchange and protein folding after being bound onto cyclophilin B. It can promote the assembly of immunoglobulin G antibody and intermolecular disulfide bonding. A controlled study examining four cigarette smokers with chronic obstructive pulmonary disease and six non-smoker controls demonstrated *PDIA4* polymorphism within the lung fibroblast endomembrane pathway as well as in the differential endoplasmic reticulum stress (ERS) response [42]. Activation of the ERS response and *PDIA4* genotype up-regulation can increase the risk of inflammatory bowel disease in children [43]. As shown in the rat model, up regulated ERS was also associated with diaphragm contractile disorders [44]. These findings help to explain our current results. Consequently, *PDIA4* appears to be a potential DEG candidate in GMD. In addition, aberrant ERS response and *PDIA4* levels are protective responses to various diseases, especially in MIRI [45]. MIRI affects the energy metabolism of cardiac cells. In cardiac muscle cells, calcium ions are regulated by the ER. During ERS and functional disorders, calcium ions can be produced in the cytoplasm by ER-calcium. This calcium overload ini-

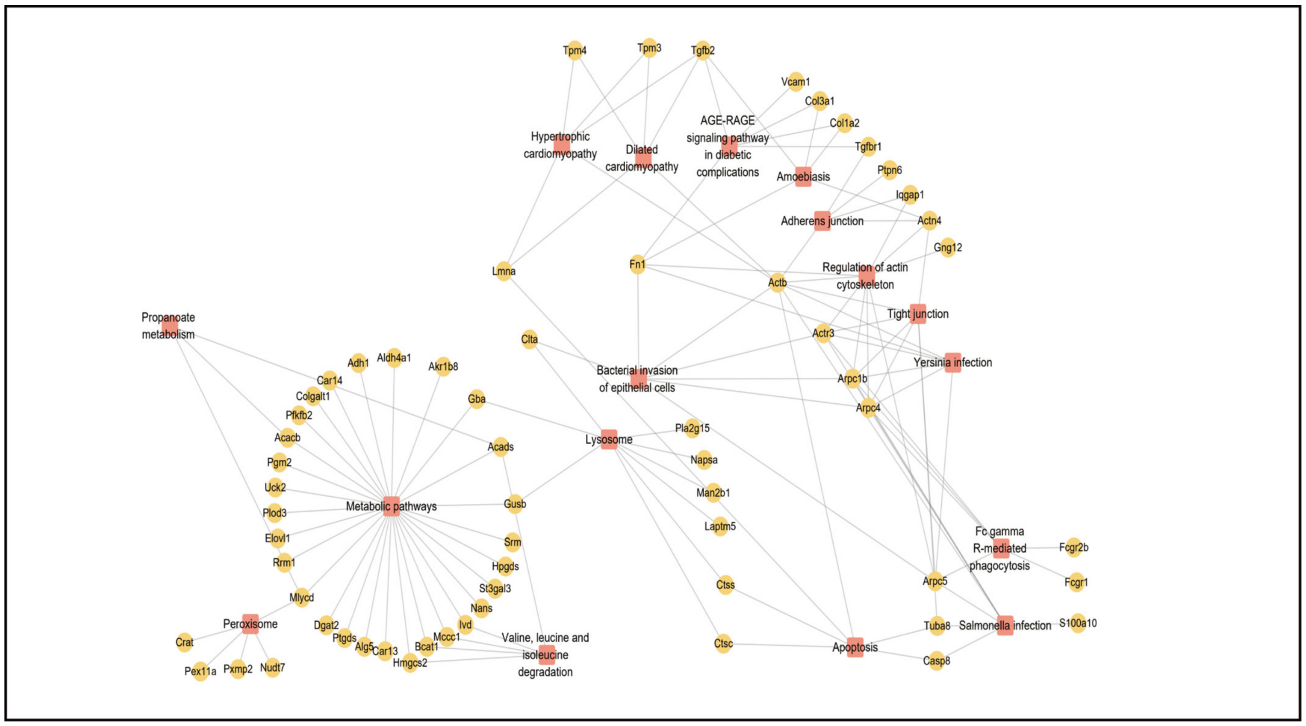

Fig. 10. Pathway-Gene Functional Network.

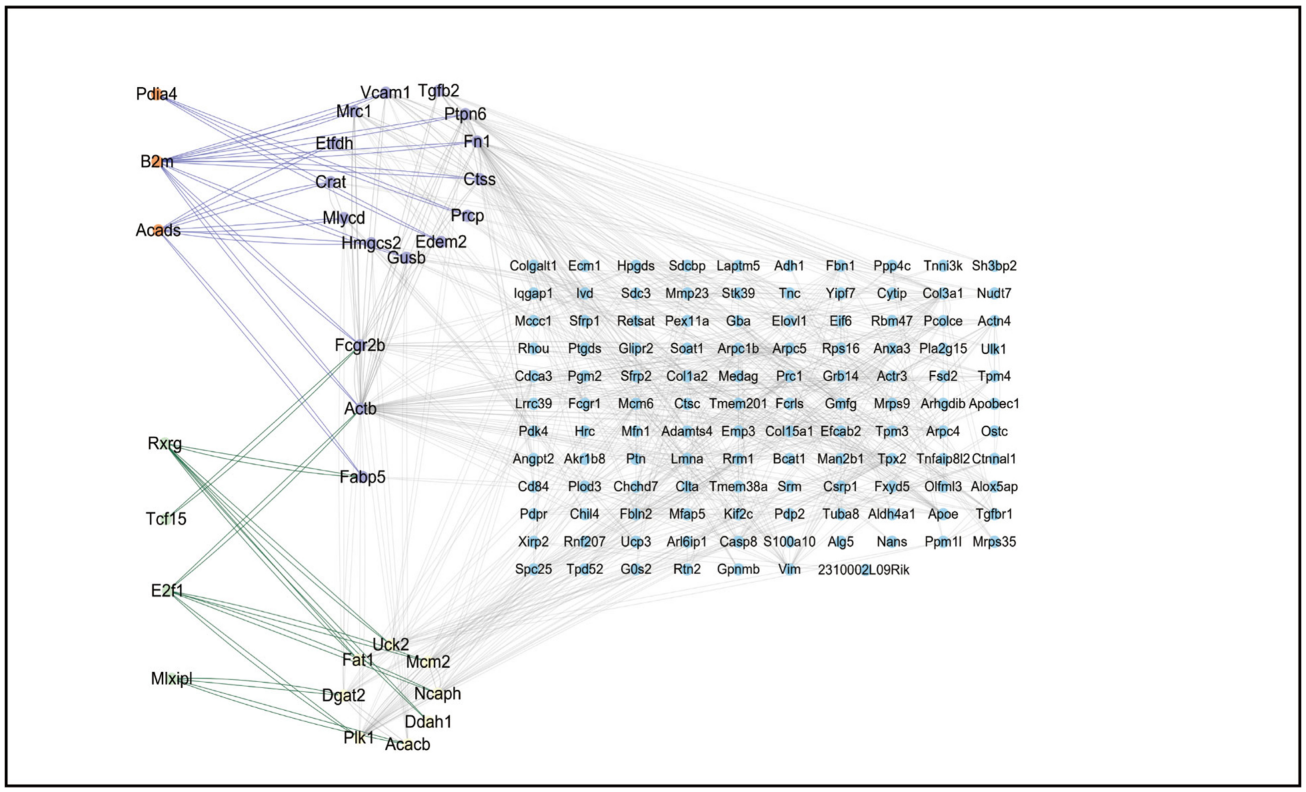

Fig. 11. TF and Pathway-Gene Functional Network.

tiates the ER-calcium-XO signaling pathway, inducing XO overexpression and activation. This event generates a sharp increase in myocardial cell reactive oxygen species (ROS); thus, causing myocardial cell death [46]. *PDIA4* is affected by ERS and unfolded protein reaction (UPR), leading to increased ROS. Ultimately, it leads to myocardial cell program death in MIRI [47]. Therefore, in MIRI-diseased individuals, *PDIA4* is critical in ERS and the UPR break-out

and endoplasmic reticulum quality control systems (ERQC) [48]. Accordingly, activation of *PDIA4* increases the risk of the GMD-driven immune response and ERS. This observation explains an interrelationship between GMD and MIRI. Moreover, three UPR branches of pathways and transcription factors are chiefly involved in GMD and MIRI. These include the pancreatic ER kinase (PKR)-like ER kinase-activating transcription factor 4, ATF6p90-ATF6p50 (activating transcription factor 6), together with IRE1-XBP1 (inositol requiring enzyme 1-X-box binding protein-1) [49–51]. In MIRI, these three pathways are essential [40]. Interestingly, *PDIA4* can be detected on platelet surface, which is the coagulation-related tissue factor activator. Platelets have been shown to accumulate and modulate related functions [52]. An arterial thrombus can be caused by aberrant thrombosis activation. *PDIA4* participates in this process during pathological conditions or injury [53]. Nevertheless, in a *PDIA4* knockdown mouse model, an extended bleeding time was found in addition to platelet impairment as well as subsequent fibrin generation [54]. This observation supports the theory of thrombosis. It mainly highlights platelet activation together with fibrin generation that is associated with changes in *PDIA4* levels, which contributes to the risk of MIRI. Despite these potential mechanisms and observations, current clinical studies remain lacking. Hence, further research is necessary to identify and verify the systemic risk factors between MIRI and GMD.

Strengths and Limitations

This study explores the transcriptomic association mechanisms of MIRI with GMD. Preliminary research has been performed in some disorders such as Alzheimer's disease and periodontitis, periimplantitis and RA, as well as periodontitis and carotid atherosclerosis. Consequently, this method should be further studies to determine the cross-talk between MIRI and GMD. Our current analysis needs further research to provide causal evidence. This comprehensive study includes TF, pathway and PPI network analysis. Our main limitations include the mouse source and low sample size in the MIRI datasets. There were just 22 acquired through merging both datasets following batch correction. Our explored model predicts the results and the tests the outcomes equally well. In addition, the characteristic gene levels were proper within the corrected GSE61592 and GSE160516 datasets. Regardless of the small sample size for the SVM module, this study suggests there is some predictive value of the data. Furthermore, the samples were analyzed to verify the reasonability of the results and augment the value of the conclusions. Two genes were the focus of the present study. Screening several genes in the whole set strengthens the significance of the findings and provides further support, such as the expression quantitative trait locus (eQTL) analysis. Additionally, single nucleotide polymorphisms (SNP) were not discussed in this work, and the available datasets did not assess SNP mutations. Therefore, the criterion for species selection in the current analysis essentially limits the applicability of our result and the ability to make definite conclusions. The *ACADS* function of alternative splicing was not discussed. This feature results in two variants that encode different isoforms. The results appear reasonable and plausible despite their inferential nature. This study identifies core cross-talk genes and TF in MIRI and GMD through an immune perspective, providing a potential new mechanism. The significance of this report is to draw attention to the potential role of the gut microbiome in determining the risk for major adverse events in patients with cardiovascular diseases. It should be noted that the results were derived by bioinformatics analysis. Further studies examining associated cell mechanisms *in vitro* or in clinical research are required to confirm these results. The current results lay the foundation for subsequent studies.

Conclusion

B2m and *PDIA4* were identified to be significantly correlated candidate cross-talk genes of MIRI with gut microbiome disorders, implying a similarity between MIRI and Gut microbiome disorders (GMD). These genes can serve as an experimental research basis for future studies.

Abbreviations

MIRI, Myocardial ischemia-reperfusion injury; GMD, Gut microbiome disorder; CAD, Coronary artery disease; GEGs, Differentially expressed genes; GEO, Gene expression omnibus; DAMPs, Damage-associated molecular patterns; MHC, Histocompatibility complex; HKG, Housekeeping gene; ERS, Endoplasmic reticulum stress; UPR, Unfolded protein reaction; ROS, Reactive oxygen species; ERQC, Endoplasmic reticulum quality control; IBD, Inflammatory bowel disease; CFs, Cardiac fibroblasts; SNP, Single nucleotide polymorphisms.

Availability of Data and Materials

The data utilized in the present work can be obtained in the published study.

Author Contributions

XJ and XL were responsible for study conception, design and planning. XJ, CL and JC acquired and analyzed the data. XJ, XX and JT interpretation of data for the work.

XJ, CL, and XX were in charge of result interpretation. XJ and JT drafted this manuscript. XJ and JC revised this manuscript. The authors read and approved the eventual manuscript. All authors contributed to editorial changes in the manuscript. All authors read and approved the final manuscript. All authors have participated sufficiently in the work to take public responsibility for appropriate portions of the content and agreed to be accountable for all aspects of the work in ensuring that questions related to its accuracy or integrity.

Ethics Approval and Consent to Participate

Not applicable.

Acknowledgment

The manuscript was released as a preprint at Research Square.

Funding

The present study was funded by a Grant from the National Natural Science Foundation of China (Grant Number 82074392).

Conflict of Interest

The authors declare no conflict of interest.

References

[1] Heusch G. Myocardial ischaemia-reperfusion injury and cardioprotection in perspective. Nature Reviews. Cardiology. 2020; 17: 773–789.

[2] Hausenloy DJ, Yellon DM. Myocardial ischemia-reperfusion injury: a neglected therapeutic target. The Journal of Clinical Investigation. 2013; 123: 92–100.

[3] Heusch G, Rassaf T. Time to Give Up on Cardioprotection? A Critical Appraisal of Clinical Studies on Ischemic Pre-, Post-, and Remote Conditioning. Circulation Research. 2016; 119: 676–695.

[4] Zhou H, Zhu P, Guo J, Hu N, Wang S, Li D, *et al*. Ripk3 induces mitochondrial apoptosis via inhibition of FUNDC1 mitophagy in cardiac IR injury. Redox Biology. 2017; 13: 498–507.

[5] Wu MY, Yiang GT, Liao WT, Tsai APY, Cheng YL, Cheng PW, *et al*. Current Mechanistic Concepts in Ischemia and Reperfusion Injury. Cellular Physiology and Biochemistry: International Journal of Experimental Cellular Physiology, Biochemistry, and Pharmacology. 2018; 46: 1650–1667.

[6] Sánchez-Hernández CD, Torres-Alarcón LA, González-Cortés A, Peón AN. Ischemia/Reperfusion Injury: Pathophysiology, Current Clinical Management, and Potential Preventive Approaches. Mediators of Inflammation. 2020; 2020: 8405370.

[7] Ghafouri-Fard S, Shoorei H, Taheri M. Non-coding RNAs participate in the ischemia-reperfusion injury. Biomedicine & Pharmacotherapy. 2020; 129: 110419.

[8] Karlsson FH, Fåk F, Nookaew I, Tremaroli V, Fagerberg B, Petranovic D, *et al*. Symptomatic atherosclerosis is associated with an altered gut metagenome. Nature Communications. 2012; 3: 1245.

[9] Vinjé S, Stroes E, Nieuwdorp M, Hazen SL. The gut microbiome as novel cardio-metabolic target: the time has come!. European Heart Journal. 2014; 35: 883–887.

[10] Kootte RS, Vrieze A, Holleman F, Dallinga-Thie GM, Zoetendal EG, de Vos WM, *et al*. The therapeutic potential of manipulating gut microbiota in obesity and type 2 diabetes mellitus. Diabetes, Obesity & Metabolism. 2012; 14: 112–120.

[11] Sirisinha S. The potential impact of gut microbiota on your health: Current status and future challenges. Asian Pacific Journal of Allergy and Immunology. 2016; 34: 249–264.

[12] Kaptoge S, Seshasai SRK, Gao P, Freitag DF, Butterworth AS, Borglykke A, *et al*. Inflammatory cytokines and risk of coronary heart disease: new prospective study and updated meta-analysis. European Heart Journal. 2014; 35: 578–589.

[13] Shreiner AB, Kao JY, Young VB. The gut microbiome in health and in disease. Current Opinion in Gastroenterology. 2015; 31: 69–75.

[14] Cerdó T, Ruiz A, Acuña I, Jáuregui R, Jehmlich N, Haange SB, *et al*. Gut microbial functional maturation and succession during human early life. Environmental Microbiology. 2018; 20: 2160–2177.

[15] Zhen Y, Zhang H. NLRP3 Inflammasome and Inflammatory Bowel Disease. Frontiers in Immunology. 2019; 10: 276.

[16] Ladinsky MS, Araujo LP, Zhang X, Veltri J, Galan-Diez M, Soualhi S, *et al*. Endocytosis of commensal antigens by intestinal epithelial cells regulates mucosal T cell homeostasis. Science (New York, N.Y.). 2019; 363: eaat4042.

[17] Yang M, Zhang Y, Ren J. Autophagic Regulation of Lipid Homeostasis in Cardiometabolic Syndrome. Frontiers in Cardiovascular Medicine. 2018; 5: 38.

[18] Yang Q, Lin SL, Kwok MK, Leung GM, Schooling CM. The Roles of 27 Genera of Human Gut Microbiota in Ischemic Heart Disease, Type 2 Diabetes Mellitus, and Their Risk Factors: A Mendelian Randomization Study. American Journal of Epidemiology. 2018; 187: 1916–1922.

[19] Li S, Zhou C, Xu Y, Wang Y, Li L, Pelekos G, *et al*. Similarity and Potential Relation Between Periimplantitis and Rheumatoid Arthritis on Transcriptomic Level: Results of a Bioinformatics Study. Frontiers in Immunology. 2021; 12: 702661.

[20] Zeng Y, Cao S, Chen M. Integrated analysis and exploration of potential shared gene signatures between carotid atherosclerosis and periodontitis. BMC Medical Genomics. 2022; 15: 227.

[21] Newman AM, Steen CB, Liu CL, Gentles AJ, Chaudhuri AA, Scherer F, *et al*. Determining cell type abundance and expression from bulk tissues with digital cytometry. Nature Biotechnology. 2019; 37: 773–782.

[22] Tan L, Tejada T, Torres R, Calvert J, Pejler G, Abrink M, *et al*. Abstract P229: Chymase-mediated Igf-1 Degradation Promotes Delayed Cell Death in Post-ischemic Hearts. Hypertension. 2016; 68: AP229–AP229.

[23] Zhao W, Wang L, Haller V, Ritsch A. A Novel Candidate for Prevention and Treatment of Atherosclerosis: Urolithin B Decreases Lipid Plaque Deposition in apoE$^{-/-}$ Mice and Increases Early Stages of Reverse Cholesterol Transport in ox-LDL Treated Macrophages Cells. Molecular Nutrition & Food Research. 2019; 63: e1800887.

[24] Kurilshikov A, van den Munckhof ICL, Chen L, Bonder MJ, Schraa K, Rutten JHW, *et al*. Gut Microbial Associations to Plasma Metabolites Linked to Cardiovascular Phenotypes and Risk. Circulation Research. 2019; 124: 1808–1820.

[25] Wang NC, Chen HW, Lin TY. Association of protein disulfide isomerase family A, member 4, and inflammation in people living with HIV. International Journal of Infectious Diseases: IJID: Official Publication of the International Society for Infectious Diseases. 2023; 126: 79–86.
[26] Feng D, Wei J, Gupta S, McGrath BC, Cavener DR. Acute ablation of PERK results in ER dysfunctions followed by reduced insulin secretion and cell proliferation. BMC Cell Biology. 2009; 10: 61.
[27] Lu H, Yang Y, Allister EM, Wijesekara N, Wheeler MB. The identification of potential factors associated with the development of type 2 diabetes: a quantitative proteomics approach. Molecular & Cellular Proteomics: MCP. 2008; 7: 1434–1451.
[28] Di Jeso B, Morishita Y, Treglia AS, Lofrumento DD, Nicolardi G, Beguinot F, *et al*. Transient covalent interactions of newly synthesized thyroglobulin with oxidoreductases of the endoplasmic reticulum. The Journal of Biological Chemistry. 2014; 289: 11488–11496.
[29] Menon S, Lee J, Abplanalp WA, Yoo SE, Agui T, Furudate SI, *et al*. Oxidoreductase interactions include a role for ERp72 engagement with mutant thyroglobulin from the rdw/rdw rat dwarf. The Journal of Biological Chemistry. 2007; 282: 6183–6191.
[30] De Santis S, Cavalcanti E, Mastronardi M, Jirillo E, Chieppa M. Nutritional Keys for Intestinal Barrier Modulation. Frontiers in Immunology. 2015; 6: 612.
[31] Yang D, Han Z, Oppenheim JJ. Alarmins and immunity. Immunological Reviews. 2017; 280: 41–56.
[32] Deguine J, Barton GM. MyD88: a central player in innate immune signaling. F1000prime Reports. 2014; 6: 97.
[33] Sedighi O, Abediankenari S, Omranifar B. Association between plasma Beta-2 microglobulin level and cardiac performance in patients with chronic kidney disease. Nephro-urology Monthly. 2014; 7: e23563.
[34] Cheung CL, Lam KSL, Cheung BMY. Serum β-2 microglobulin predicts mortality in people with diabetes. European Journal of Endocrinology. 2013; 169: 1–7.
[35] Pecoits-Filho R, Lindholm B, Stenvinkel P. The malnutrition, inflammation, and atherosclerosis (MIA) syndrome – the heart of the matter. Nephrology, Dialysis, Transplantation: Official Publication of the European Dialysis and Transplant Association - European Renal Association. 2002; 17: 28–31.
[36] Kals J, Zagura M, Serg M, Kampus P, Zilmer K, Unt E, *et al*. β2-microglobulin, a novel biomarker of peripheral arterial disease, independently predicts aortic stiffness in these patients. Scandinavian Journal of Clinical and Laboratory Investigation. 2011; 71: 257–263.
[37] Wu HC, Lee LC, Wang WJ. Associations among Serum Beta 2 Microglobulin, Malnutrition, Inflammation, and Advanced Cardiovascular Event in Patients with Chronic Kidney Disease. Journal of Clinical Laboratory Analysis. 2017; 31: e22056.
[38] Molenaar B, Timmer LT, Droog M, Perini I, Versteeg D, Kooijman L, *et al*. Single-cell transcriptomics following ischemic injury identifies a role for B2M in cardiac repair. Communications Biology. 2021; 4: 146.
[39] Psarras S, Beis D, Nikouli S, Tsikitis M, Capetanaki Y. Three in a Box: Understanding Cardiomyocyte, Fibroblast, and Innate Immune Cell Interactions to Orchestrate Cardiac Repair Processes. Frontiers in Cardiovascular Medicine. 2019; 6: 32.
[40] Shao L, Zhang Y, Pan X, Liu B, Liang C, Zhang Y, *et al*. Knockout of beta-2 microglobulin enhances cardiac repair by modulating exosome imprinting and inhibiting stem cell-induced immune rejection. Cellular and Molecular Life Sciences: CMLS. 2020; 77: 937–952.
[41] Krzystek-Korpacka M, Diakowska D, Bania J, Gamian A. Expression stability of common housekeeping genes is differently affected by bowel inflammation and cancer: implications for finding suitable normalizers for inflammatory bowel disease studies. Inflammatory Bowel Diseases. 2014; 20: 1147–1156.
[42] Weidner J, Jarenbäck L, Åberg I, Westergren-Thorsson G, Ankerst J, Bjermer L, *et al*. Endoplasmic reticulum, Golgi, and lysosomes are disorganized in lung fibroblasts from chronic obstructive pulmonary disease patients. Physiological Reports. 2018; 6: e13584.
[43] Tufo G, Jones AWE, Wang Z, Hamelin J, Tajeddine N, Esposti DD, *et al*. The protein disulfide isomerases PDIA4 and PDIA6 mediate resistance to cisplatin-induced cell death in lung adenocarcinoma. Cell Death and Differentiation. 2014; 21: 685–695.
[44] Jiao G, Hao L, Wang M, Zhong B, Yu M, Zhao S, *et al*. Up-regulation of endoplasmic reticulum stress is associated with diaphragm contractile dysfunction in a rat model of sepsis. Molecular Medicine Reports. 2017; 15: 366–374.
[45] Winship AL, Sorby K, Correia J, Rainczuk A, Yap J, Dimitriadis E. Interleukin-11 up-regulates endoplasmic reticulum stress induced target, PDIA4 in human first trimester placenta and *in vivo* in mice. Placenta. 2017; 53: 92–100.
[46] Zhang Y, Zhou H, Wu W, Shi C, Hu S, Yin T, *et al*. Liraglutide protects cardiac microvascular endothelial cells against hypoxia/reoxygenation injury through the suppression of the SR-Ca(2+)-XO-ROS axis via activation of the GLP-1R/PI3K/Akt/survivin pathways. Free Radical Biology & Medicine. 2016; 95: 278–292.
[47] Zhu P, Hu S, Jin Q, Li D, Tian F, Toan S, *et al*. Ripk3 promotes ER stress-induced necroptosis in cardiac IR injury: A mechanism involving calcium overload/XO/ROS/mPTP pathway. Redox Biology. 2018; 16: 157–168.
[48] Bertolotti A, Zhang Y, Hendershot LM, Harding HP, Ron D. Dynamic interaction of BiP and ER stress transducers in the unfolded-protein response. Nature Cell Biology. 2000; 2: 326–332.
[49] Zhang K, Kaufman RJ. Signaling the unfolded protein response from the endoplasmic reticulum. Journal of Biological Chemistry. 2004; 279: 25935–25938.
[50] Zhang K, Kaufman RJ. The unfolded protein response: a stress signaling pathway critical for health and disease. Neurology. 2006; 66: S102–S109.
[51] Zhang K, Kaufman RJ. From endoplasmic-reticulum stress to the inflammatory response. Nature. 2008; 454: 455–462.
[52] Stopa JD, Zwicker JI. The intersection of protein disulfide isomerase and cancer associated thrombosis. Thrombosis Research. 2018; 164: S130–S135.
[53] Essex DW, Wu Y. Multiple protein disulfide isomerases support thrombosis. Current Opinion in Hematology. 2018; 25: 395–402.
[54] Zhou J, Wu Y, Chen F, Wang L, Rauova L, Hayes VM, *et al*. The disulfide isomerase ERp72 supports arterial thrombosis in mice. Blood. 2017; 130: 817–828.